

# DEVELOPMENT OF A NEW BEAM-ENERGY-SPREAD MONITOR USING MULTI-STRIPLINE ELECTRODES

T. Suwada\*, M. Satoh and K. Furukawa, KEK, Tsukuba, Ibaraki 305-0801, Japan

## Abstract

A nondestructive beam-energy-spread monitor (BESM) using multi-stripline electrodes has been newly developed in order to measure and control the energy spread of a single-bunch electron beam at the 180-degree arc with a beam energy of 1.7 GeV in the KEKB injector linac. A proof-of-principle experiment was performed to verify the function of the BESM. The result shows that taking into account the second-order moment derived from the multipole-moment analysis, the energy spreads are estimated to be  $0.150 \pm 0.007\%$  and  $0.264 \pm 0.004\%$  for the electron beams with charges of 0.9 and 8 nC/bunch at the rf phase of the energy-spread minimum, respectively.

## 1 INTRODUCTION

The KEK B-Factory (KEKB) project [1] is in progress for testing CP violation in the decay of B mesons. KEKB is an asymmetric electron-positron collider comprising 3.5-GeV positron and 8-GeV electron rings. Since KEKB is a factory machine, well-controlled operation of the KEKB injector linac [2] is required for keeping the injection rate as high as possible and for maintaining stable operation. For this purpose, beam diagnostic and monitoring tools are essential. The energy spread of the primary electron beam for positron generation is often increased due to a long-term phase drift of high-power and booster klystrons. Thus, beam diagnostic and monitoring tools are required to cure the beam energy spread; furthermore, those are expected to control the longitudinal wakefields of the high-current primary electron beam pulse-by-pulse, especially at large energy dispersion sections.

The BESM with multi-stripline electrodes is one of very useful monitoring tools for satisfying such requirements, since it can measure the energy spread derived from a quadrupole moment of an electron beam. This monitor was designed based on a numerical analysis by applying the multipole moments of the electromagnetic field generated by a charged beam [3]. The BESM detects the spread of transverse beam widths at a large energy dispersion section by measuring any variation of the electromagnetic field distribution induced on the multi-stripline electrodes of the monitor. In this report the authors not only present a clear experimental verification of this analysis based on the previous works [4, 5], but also demonstrate that the second-order moment of an electron beam can be nondestructively measured by the BESM, depending on the variation of the energy spread. The BESM will enable to acquire beam characteristics of two beam bunches in an rf pulse in which

scheme they are injected to the rings simultaneously.

## 2 MULTIPOLE-MOMENT ANALYSIS OF A CHARGED BEAM

For a conducting round duct, the image charges induced by a line charge can be solved as a boundary problem in which the electrostatic potential is equal on the duct [6] (also see Ref. [7]). The formula for the image charge density  $j$  is given by

$$j(r, \phi, R, \theta) = \frac{I(r, \phi)}{2\pi R} \frac{R^2 - r^2}{R^2 + r^2 - 2rR \cos(\theta - \phi)}, \quad (1)$$

where  $I$  is the line charge,  $(r, \phi)$  and  $(R, \theta)$  are the polar coordinates of the line charge and the pickup point on the duct, respectively, and  $R$  is the duct radius. Assuming the transverse  $r$ -distribution  $\rho(r)$  of a traveling charged beam, the total image charge  $J$  is formulated by integrating the image charge density with a weight of the transverse distribution inside the duct area,

$$J(R, \theta) = \int_0^R \int_0^{2\pi} j(r, \phi, R, \theta) \rho(r) r dr d\phi. \quad (2)$$

It is easily expanded by a power series,

$$\begin{aligned} J(R, \theta) &= \frac{I_b}{2\pi R} \left\{ 1 + \frac{2}{R} (\langle x \rangle \cos \theta + \langle y \rangle \sin \theta) \right. \\ &\quad + \frac{2}{R^2} [(\langle x^2 \rangle - \langle y^2 \rangle) + \langle x \rangle^2 - \langle y \rangle^2] \cos 2\theta \\ &\quad + 2(\langle xy \rangle + \langle x \rangle \langle y \rangle) \sin 2\theta \\ &\quad \left. + \text{higher orders} \right\}, \end{aligned} \quad (3)$$

where  $I_b$  is the beam charge,  $\langle x \rangle$  and  $\langle y \rangle$  are the charge center of gravity of the beam,  $\langle x^2 \rangle$  and  $\langle y^2 \rangle$  are the horizontal and vertical mean square half widths of the beam in the  $x$  and  $y$  directions, and  $\langle xy \rangle$  is the x-y coupling in the transverse plane, respectively. A transverse beam-width measurement is performed to detect the second-order (quadrupole) moment  $J_q$  at the least orders. The quadrupole moment is described by using the following eight-pickup amplitudes [ $V_i$  ( $i=1-8$ )] of the BESM:

$$\begin{aligned} J_q &\equiv \int_0^{2\pi} J(R, \theta) \cos 2\theta d\theta / \int_0^{2\pi} J(R, \theta) d\theta, \\ &= \frac{1}{R^2} (\langle x^2 \rangle - \langle y^2 \rangle) + \langle x \rangle^2 - \langle y \rangle^2, \\ &\simeq \frac{\sum_{i=1}^8 V_i \cos 2\theta}{\sum_{i=1}^8 V_i}, \end{aligned} \quad (4)$$

\* e-mail:tsuyoshi.suwada@kek.jp

Normalization by summing the eight-pickup amplitudes needs to cancel out the beam charge fluctuations due to any beam measurement jitter. It is understood that the quadrupole moment is related to the transverse beam widths, while it also depends on the beam positions.

### 3 BEAM ENERGY-SPREAD MONITOR

Figure 1 show schematic cross-sectional drawings of the BESM. The mechanical design parameters are summarized in Table 1. The BESM is a conventional monitor with eight-stripline electrodes fabricated from stainless steel (SUS304) with  $\pi/8$  rotational symmetry. The stripline length  $L$  was determined to be as long as could possibly be installed into the limited spaces in the beam line so as to increase the signal-to-noise ratio. The inner and outer radii,  $R_1$  and  $R_2$ , and the angular width  $\alpha$  of the electrode were chosen so as to comprise a  $50\text{-}\Omega$ -transmission line. The eight pickups with a relatively narrow angular width of 15 degree are mounted with a tilt of  $\pi/8$  rad at the symmetrical polar coordinates in order to avoid any direct impinging of synchrotron radiation and off-energy electrons to the electrode surfaces at a large energy dispersion section.

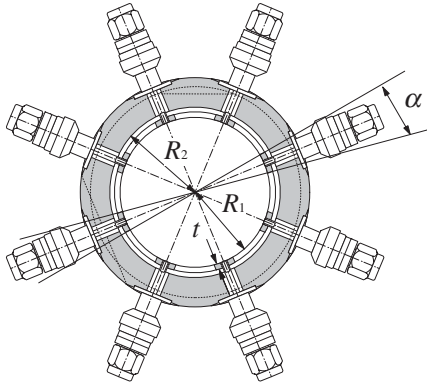


Figure 1: Schematic cross-sectional drawing of the beam energy-spread monitor.

Table 1: Mechanical design parameters of the BESM.

Mechanical parameter	
Innner radius $R_1$ (mm)	20.6
Outer raidus $R_2$ (mm)	23.4
Electrode angular width $\alpha$ (deg)	15
Electrode thickness $t$ (mm)	1.5
Electrode length $l$ (mm)	132.5
Total length $L$ (mm)	283

### 4 BEAM TEST

Beam experiments using single-bunch electron beams of 0.9 and 8 nC/bunch were carried out under the nominal operation condition at the 180-degree arc after sector B

where the beam energy is 1.7 GeV. The layout of the beam line is described elsewhere [2]. The multipole moments of the electron beam were measured by the BESM while the transverse spatial profiles of the beam were directly measured by a fluorescent screen monitor (SC) installed behind the BESM with a beam-synchronous CCD camera and a video-image frame grabber in order to calibrate the BESM results at a rate of 1 Hz.

The transverse beam widths at the locations of these monitors were controlled by changing the rf phase of the booster klystron at sector B. The BPMs located at sectors A, B and the arc monitored the beam positions and charges of the beam in order to control the beam positions and energy stably through the feedback systems without any beam loss during the experiment.

The beam experiments with the BESM were performed by measuring the quadrupole moment of the 0.9-nC electron beam, as a function of the horizontal ( $x$ ) and vertical ( $y$ ) beam positions. In this measurement the rf phase of the booster klystron at sector B was fixed to reduce the energy spread to its minimum with the beam-orbit and energy feedbacks at sector B off. The beam positions at the BESM were controlled by the field strength of upstream x and y steering magnets. The quadrupole moments of the 0.9-nC and 8-nC electron beam depending on the rf phase of the booster klystron were also measured while the beam positions of the electron beam were fixed at the center of the BESM with the beam-orbit and energy feedbacks on. One data point of the BESM was obtained by averaging 200 successive data with the statistical errors after the position dependence was corrected.

### 5 EXPERIMENTAL RESULTS

Figure 2 shows the variations of the quadrupole moment depending on the field strength of the upstream x steering magnet for the 0.9-nC electron beam with and without the beam-position corrections. It is clearly shown that after the corrections of the beam position, the quadrupole moment is constant over the measured range of the field strength of the steering magnet within the estimated errors. Figure 3 shows the variations of the quadrupole moment for the 0.9-nC and 8-nC electron beam depending on the rf phase of the booster klystron after the beam-position correction. For the 0.9-nC electron beam the beam-width data directly measured by the screen monitor are also added in order to compare the BESM data after the beam-profile correction on the transverse distributions.

The BESM data are related to the SC data by,

$$\langle x^2 \rangle - \langle y^2 \rangle = f (X^2 - Y^2) + g, \quad (5)$$

where  $X$  and  $Y$  are the transverse beam widths measured by the screen monitor in HWHM,  $g$  is a fitting parameter caused by the gain imvalance and the geometrical errors of the eight pickups of the BESM, and the parameter  $f$  is the beam-profile correction factor depending upon the transverse distributions of the electron beam (see Ref. [7]). The

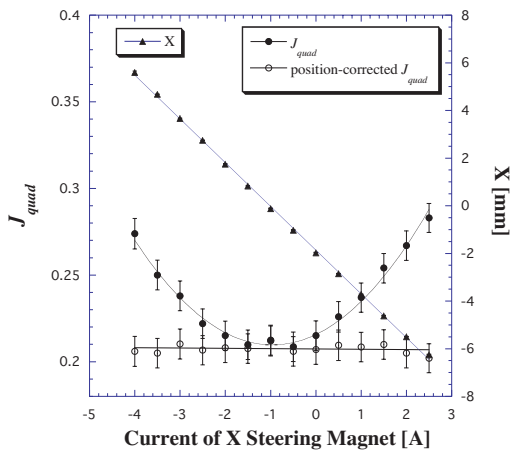


Figure 2: Variations of the quadrupole moment depending on the field strength of the horizontal upstream steering magnet for the 0.9-nC electron beam.

result shows that the transverse beam profile is approximately well described not by a Gaussian function, but by a parabolic function. The BESM data agree well with the corrected SC data within the estimated errors over the measured region of the rf phase.

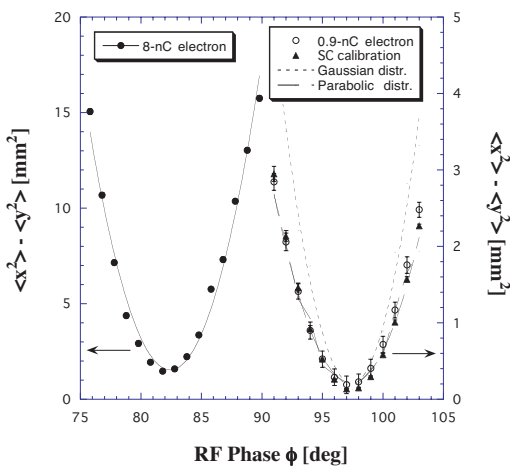


Figure 3: Variations of the quadrupole moment depending on the rf phase of the booster klystron.

Assuming that the vertical dispersion  $\eta_y$  is zero at the BESM, the energy spread  $\Delta E$  of the electron beam can be estimated from the transverse beam widths along with the optics parameters ( $\beta$  functions and horizontal dispersion  $\eta_x$ ) and the transverse emittances as follows:

$$\langle x^2 \rangle - \langle y^2 \rangle \simeq \beta_x \epsilon_x + (\eta_x \Delta E / E)^2 - \beta_y \epsilon_y + g, \quad (6)$$

where  $g$  is the same parameter as defined in Eq.(5), and the transverse emittances,  $\epsilon_x$  and  $\epsilon_y$ , were measured by wire scanners at the end of sector B (see Ref. [7]). The result shows that the obtained energy spreads are  $0.150 \pm 0.007\%$  and  $0.264 \pm 0.004\%$  for the electron beams with charges of 0.9 and 8 nC/bunch at the rf phase of the energy-spread minimum, respectively.

minimum, respectively. The resolution for the energy-spread measurement is on the order of  $10^{-3}$ , depending on the beam charge. Figure 4 shows the time trend of the measured quadrupole moment and the rf phase of the booster klystron during six hours, where the BESM data were obtained pulse-by-pulse and the rf phase data were taken every 1.5 minute. The good agreement between these two data is a clear demonstration of the principal function of the BESM.

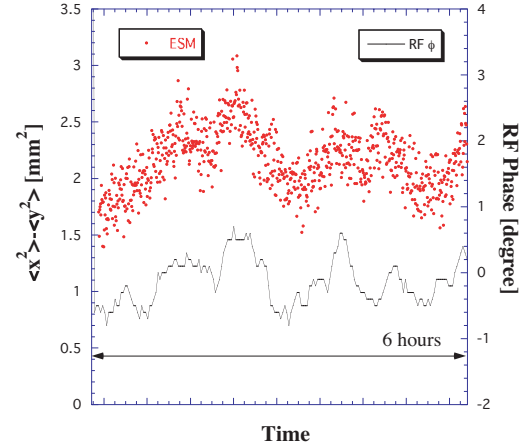


Figure 4: Time trend of the quadrupole moment and the rf phase of the booster klystron.

## 6 CONCLUSIONS

The second-order moments of single-bunch electron beams were accurately measured by the nondestructive beam-energy-spread monitor with multi-stripline electrodes at the injector linac. The result shows that the analyzed energy spreads were  $0.150 \pm 0.007\%$  and  $0.264 \pm 0.004\%$  for electron beams with charges of 0.9 and 8 nC/bunch at the rf phase of the energy-spread minimum, respectively. The authors have a plan to investigate beam characteristics of two beam bunches in the two beam bunch injection scheme in the nominal operation mode.

## 7 REFERENCES

- [1] S. Kurokawa and E. Kikutani, Nucl. Instrum. Methods Phys. Res. A499 (2003) pp.1-7.
- [2] I. Abe *et al.*, Nucl. Instrum. Methods Phys. Res. A499 (2003) pp.167-190.
- [3] T. Suwada, *LINAC2000, Monterey, California, U.S.A., 2000*, pp.199-201.
- [4] R. H. Miller, J. E. Clendenin, M. B. James and J. C. Sheppard, *HEAC'83, Fermilab, U.S.A., 1983*, pp.602-605.
- [5] T. Suwada, Jpn. J. Appl. Phys. 40 (2001) pp.890-897.
- [6] J. D. Jackson, *Classical Electrodynamics* (John Wiley & Sons, New York, 1975) 2nd ed., p.54.
- [7] T. Suwada, M. Satoh and K. Furukawa, Phys. Rev. ST Accel. Beams 6 032801 (2003).